Published in final edited form as:
J Control Release. 2014 February 28; 176: 76–85. doi:10.1016/j.jconrel.2013.12.018.

Development and Evaluation of Transferrin-Stabilized Paclitaxel Nanocrystal Formulation

Ying Lu[1], **Zhao-hui Wang**[1], **Tonglei Li**[1], **Helen McNally**[2], **Kinam Park**[1,3,*], and **Michael Sturek**[4]

[1]Purdue University, Department of Industrial and Physical Pharmacy, West Lafayette, IN 47907, U.S.A.

[2]Purdue University, Electrical and Computer Engineering Technology, West Lafayette, IN 47907, U.S.A.

[3]Purdue University, Weldon School of Biomedical Engineering, West Lafayette, IN 47907, U.S.A.

[4]Indiana University School of Medicine, Department of Cellular & Integrative Physiology, Indianapolis, IN 46202, U.S.A.

Abstract

The aim of the present study was to prepare and evaluate a paclitaxel nanocrystal-based formulation stabilized by serum protein transferrin in a non-covalent manner. The pure paclitaxel nanocrystals were first prepared using an antisolvent precipitation method augmented by sonication. The serum protein transferrin was selected for use after evaluating the stabilizing effect of several serum proteins including albumin and immunoglobulin G. The formulation contained approximately 55~60% drug and was stable for at least 3 months at 4 °C. *In vivo* antitumor efficacy studies using mice inoculated with KB cells demonstrate significantly higher tumor inhibition rate of 45.1% for paclitaxel-transferrin formulation compared to 28.8% for paclitaxel nanosuspension treatment alone. Interestingly, the Taxol® formulation showed higher antitumor activity than the paclitaxel-transferrin formulation, achieving a 93.3% tumor inhibition rate 12 days post initial dosing. However, the paclitaxel-transferrin formulation showed a lower level of toxicity, which is indicated by steady increase in body weight of mice over the treatment period. In comparison, treatment with Taxol® resulted in toxicity issues as body weight decreased. These results suggest the potential benefit of using a serum protein in a non-covalent manner in conjunction with paclitaxel nanocrystals as a promising drug delivery model for anticancer therapy.

Keywords

Paclitaxel; nanocrystal; albumin; transferrin; antitumor efficacy; Taxol; in vivo testing

1. Introduction

Paclitaxel is a naturally occurring diterpenoid extracted from the bark of the Pacific yew tree (*Taxus brevifolia*) [1]. In clinical trials paclitaxel has demonstrated antitumoral activity through high-affinity binding to microtubules, stabilizing and enhancing tubulin polymerization and suppression of spindle microtubule dynamics [2–4]. These activities

Address correspondence: Kinam Park, Purdue University, Weldon School of Biomedical Engineering, 206 S. Martin Jischke Drive, West Lafayette, IN 47907, kpark@purdue.edu.

effectively inhibit cell mitosis, motility and intracellular transport, which lead to apoptotic cell death. Unfortunately, clinical advances of paclitaxel in its natural form have been limited by its physicochemical property, more specifically its poor aqueous solubility (~0.3 μg/ml) [5]. The lack of a functional group in the structure of the paclitaxel molecule makes chemical modification of the natural molecule to increase solubility difficult [6]. Therefore, the selection of appropriate delivery platforms to delivery paclitaxel is particularly crucial to the clinical advancement of this antitumor compound.

Various paclitaxel delivery systems have been investigated to improve the solubility and pharmacological properties of paclitaxel, including micelles, liposomes, microparticles, nanoparticles and the use of cosolvents and cyclodextrins [7–10]. The most widely known delivery platform is a cosolvent system consisting of a 50:50 mixture of Cremophor EL® (a polyoxyethylated castor oil) and ethanol. The corresponding formulation (Taxol® or generic equivalents) consists of paclitaxel dissolved at a concentration of 6 mg/ml in the aforementioned cosolvent system, and is administered intravenously following dilution with normal saline or 5% dextrose solution[11]. While this approach overcomes the limiting solubility of paclitaxel, the use of Cremophor EL has been associated with serious and dose-limiting toxicities. More specifically, Cremophor EL has been known to leach plasticizers from standard intravenous tubing, releasing di(2-ethylhexyl)phthalate (DEHP)[1]. The infusion of DEHP has been demonstrated to produce a histamine release and result in hypersensitivity reactions in 20~40% of unpremedicated patients in phase I clinical trials[12]. Furthermore, Cremophor EL has also been associated with hyperlipidemia, erythrocyte aggregation, sensory neuropathy and neutropenia [13–15]. Clearly there is a need to develop alternative delivery systems for paclitaxel that enhance drug solubility while eliminating adverse reactions.

A possible alternative delivery system for paclitaxel is a nanosuspension formulation. A nanosuspension consists of nanosized, crystalline particles that may or may not be stabilized by a suitable stabilizer or multiple stabilizers [16, 17]. Nanosuspension formulations of several drugs are already marketed, including Rapamune® (sirolimus), Emend® (aprepitant) and Tricor® (fenofibrate)[18]. There are several advantages to using nanosuspension formulations for delivery of anticancer agents such as paclitaxel: (i) nanosized particles can enhance dissolution velocity and saturation solubility of a poorly soluble drug as predicted by the Noyes-Whitney and Ostwald-Freundlich principles, which usually leads to increasing bioavailability [19]; (ii) nanocrystalline particles require no solubilizing chemicals, therefore it's possible to achieve high drug loading [20] and (iii) nanosized particles may lead to better antitumor efficacy via the enhanced permeation and retention effect, which is associated with extravasation and retention of particles in the vicinity of the tumor [21]. Given these advantages, there has been increasing interest in formulating anticancer drugs into nanosuspension formulations.

Techniques to produce nanosized crystalline particles can be categorized into top-down technologies such as milling and high pressure homogenization, and bottom-up methods such as precipitation and self-assembly[22–26]. Commonly used top-down methods have limitations such as the need for repeated milling cycles, as well as the potential for contamination from erosion of milling materials. High pressure homogenization in particular requires a relatively high number of cycles to achieve sufficient particle size reduction, which increases cost and risk of contamination and product degradation. The precipitation method involves dissolving the drug in a solvent and then adding it to a non-solvent, which leads to the production of finely dispersed, precipitated drug. Compared to top-down techniques, a major advantage of the precipitation method is its relative simplicity and low cost. However, since solvents are used in this process, solvent choice and removal are important issues to take into consideration. Furthermore, the size of the nanocrystals can be

hard to control. The stability of the nanocrystals is a major concern; particle aggregation and growth can occur and should be prevented[27].

To stabilize nanocrystal formulations, typical strategy includes the addition of hydrophilic polymers and/or surfactants to the nanosuspensions. Stabilization is achieved through repulsion by either steric or electrostatic hindrance, whereby these polymers or surfactants adsorbed onto the surface of the nanocrystals and/or alter the dielectric constant of the liquid environment. Commonly used stabilizers include semi-synthetic non-ionic polymer such as hydroxypropyl methylcellulose (HPMC), synthetic linear polymers such as polyvinylpyrrolidone (PVP) and polyethylene glycol (PEG 400), synthetic copolymers such as Pluronic® F127 and F68, ionic surfactants such as sodium dodecyl sulfate (SDS) and non-ionic surfactants such as polysorbate esters Tween® 20 and Tween® 80 [28].

Another possible strategy is the use of proteins as stabilizers. In particular, proteins found naturally in the body, such as serum proteins, present an attractive alternative to the traditional stabilizers. Proteins have been widely used in the past as emulsifiers that help to stabilize oil-in-water emulsions [29]. Theoretically, serum proteins, such as albumin, may also provide a stabilizing effect to nanocrystals because they have been known to adsorb onto hydrophobic surfaces with a certain degree of binding affinity and therefore may provide steric hindrance to nanocrystal aggregation and growth [30, 31]. In preliminary studies, it was found that the presence of serum in a drug nanosuspension resulted in effective inhibition of particle size increase during subsequent centrifugation and drying procedures compared to the absence of serum in nanosuspension (data not shown). The presence of serum was also found to inhibit aggregation of nanocrystals in an aqueous buffer environment. Therefore, it seems that serum proteins may be likely candidates for stabilizing nanosuspensions. In addition to stabilizing effects, a potential advantage of using serum proteins over traditional polymer or surfactant-based stabilizers is the ability to bind certain membrane proteins that are often present in tumorous cells [32]. The ability to bind receptor proteins present in tumor cell membranesis a property that is particularly valuable in antitumor treatments since it may facilitate targeting of anticancer drugs to the tumor site [33].

The present study describes the development and evaluation of paclitaxel nanosuspension formulations with serum protein as a stabilizer. Serum protein was successfully fractionated into different fractions and analyzed for maximal stabilizing effect. The major components of the most effective fraction (as determined by SDS-PAGE) were then analyzed further as potential stabilizers for the paclitaxel nanosuspension formulation. To the authors' knowledge, the formulation described herein is a novel approach to the development of nanoparticle-based antitumor treatment in the sense that serum protein was used as a stabilizer in a non-covalent manner. Human KB nasopharyngeal epidermal carcinoma cells and SKOV-3 ovarian cancer cell models were used to assess the *in vitro* antitumor efficacy of the formulation. The data obtained from KB cells were compared to data from mice models to assess the *in vivo* performance of the paclitaxel nanosuspension formulation.

2. Materials and methods

2.1.Preparation of paclitaxel nanocrystals

Paclitaxel (PTX) was supplied by Samyang Genex Corporation (Daejeon, Korea) Nanocrystals were prepared by an antisolvent precipitation process supplemented by sonication. In brief, 1 ml solution of PTX was injected into deionized water with or without polymers or surfactants at 4°C under rapid stirring (1200 rpm) and intense sonication (FS20D Bath Sonicator, Fisher Scientific, Waltham, MA). The solvents evaluated were methanol, ethanol, methylene chloride (DCM), ethyl acetate (EA) and dimethyl sulfoxide

(DMSO) (Sigma Aldrich, St. Louis, MO). The polymers and surfactants were chosen from HPMC (Hercules Inc., Wilmington, DE), PVP (Dow Chemical Company, Midland, MI), PEG 400 (Sigma Aldrich, St. Louis, MO), Pluronic F127 and F68 (BASF, Florham Park, NJ),SDS (Sigma Aldrich, St. Louis, MO), Tween 20 and Tween 80 (Sigma Aldrich, St. Louis, MO). Processing conditions (solvent-to-antisolvent ratio, stirring speed, mixing time) were evaluated for their ability to produce stable nanosized particles less than 300 nm within 20 minutes of processing. A detailed flow chart of how the final process parameters were optimized is presented in Figure 1.

2.2. Preparation of formulation

Serum protein fractionation—Human serum (type AB, male, Sigma Aldrich, St Louis, MO) was separated into several fractions according to a modified cold ethanol plasma-protein precipitation process[34, 35]. In brief, three stock solutions were prepared: 4 M sodium acetate buffer, 10 M acetic acid and 53.3% (v/v) ethanol-water mixture were prepared by standard practices. Each fraction of serum proteins was obtained by carefully controlling the ionic strength, pH and polarity of the processing buffer environment. The ionic strength, pH and polarity of buffers were controlled by varying composition of the three stock solutions from above. Each fraction was separated from the rest by centrifugation at 3500× *g* for 10 minutes. Serum proteins were separated using the procedure described in Figure 1 into a total of 4 fractions and freeze dried. The fractions were stored at −20 °C until further use.

SDS-Polyacrylamide gel electrophoresis—The serum protein fractions were characterized for their composition using SDS-PAGE by standard established procedures. Polyacrylamide gels composed of 10% stacking and 5% resolving gel were prepared. After electrophoresis, the gels were stained by Coomassie Blue and then de-stained with methanol and glacial acetic acid. The molecular weight of the protein bands was determined by electrophoresis of a standard molecular weight marker protein (Bio-Rad, Hercules, CA).

Formulation development—PTX nanocrystals were prepared according to procedures outlined previously in this manuscript. A certain amount of PTX nanocrystals was suspended in deionized water and added to a solution of serum protein fractions 1–4, serum protein human serum albumin (HSA), transferrin (Trf) or immunoglobulin G (IgG) (Sigma-Aldrich, St Louis, MO) in a drop-wise fashion under gentle stirring. When the addition of PTX nanosuspension was complete, the mixture continued to be gently stirred for another 15 minutes before centrifugation at 4 °C andfreeze drying. The formulation composition (PTX to serum fraction or serum protein ratio) was evaluated for its ability to produce stable nanosuspensions with minimal particle size change after freeze drying. In addition, the final target formulation should have a composition of at least 25% drug loading.

2.3. Characterization of formulation

Particle size and zeta potential analysis—The mean particle size and the polydispersity index (PDI) were measured by dynamic light scattering (90Plus Particle Size Analyzer, Brookhaven Instruments, Holtsville, NY). Zeta potential (ZP) was measured by the same instrument equipped with a zeta potential analyzer. For sample preparation, approximately 1 mg of freeze dried sample was suspended in 4 ml of redistilled water and vortexed for 5 minutes followed by sonication for 30 seconds to disperse the sample throughout the medium. A suitable scattering intensity was selected for collecting final measurements. The particle size, PDI and ZP were measured in triplicate.

Particle morphology—Particle morphology was characterized by scanning electron microscope (SEM) (FEI Nova™ NanoSEM, FEI, Hillsboro, OR) and atomic force

microscope (AFM) (Bioscope Catalyst®, Bruker Instruments, MA). Samples for characterization by SEM were prepared by carefully depositing a small amount of freeze-dried sample onto the surface of aluminum stubs and sputter coating with a conductive layer of platinum for 1 minute under vacuum conditions.

Physical state characterization—The solid form of pure PTX and formulation were characterized by powder X-ray diffraction (PXRD) (Siemens Bruker D5000, Bruker AXS, Madison, WI) using CuK radiation at 30 mA and 45 kV (scanning rate 0.4°/min), and diffraction angles (2θ) of 3–40°. Samples for PXRD were prepared by crushing a desired amount of pure or freeze-dried nanosuspension with mortar and pestle before adding to the sample holder. Excess powder sample was scraped away and the surface of the powder sample was leveled with a glass slide.

Storage stability study—PTX formulation was stored at 4°C over a period of 3 months. Particle size, PDI and ZP of the storage samples were measured at 0, 1, 2 and 3 months. In addition, solid form characterization using PXRD was carried out for samples stored for 3 months at 4°C for physical stability assessments.

Drug content—The amount of PTX in the formulation was determined by accurately measuring out 5 mg of freeze-dried nanosuspension formulation and re-suspending in 1 ml of deionized water by vortexing and sonication. Approximately 10 ml of coldethanol was then added to the suspension and vigorously mixed by vortexing and sonication for 20 minutes. Following centrifugation of this solution for 5 minutes at 5,000 rpm, the supernatant containing dissolved PTX was collected. The pellet containing precipitated protein was washed with cold ethanol. The centrifugation and washing procedures were repeated at least 3 times, each time the supernatant was collected and combined. The PTX solution was rotary evaporated then re-dissolved in 10 ml of mobile phase for analysis by HPLC. The HPLC system (Agilent 1100 series, Agilent, Santa Clara, CA) was equipped with an autosampler, in-line degasser and an UV absorbance detector. Separation was achieved using a Phenomenex C-18 (250 mm × 4.6 mm) analytical column (Torrance, CA) at a flow rate of 1 ml/min, a detection wavelength of 228 nm and an injection volume of 20 μl. The mobile phase consisted of water, acetonitrile and methanol (40:30:30 v/v). Samples and mobile phase were filtered through a 0.22 μm syringe filter and a 0.48 μm membrane filter respectively prior to use. Drug content was calculated using the following equation:

$$Drug\ content = \frac{Mass\ of\ PTX}{Mass\ of\ dry\ formulation} \times 100\%$$

***In vitro* dissolution—**PTX release was carried out by suspending an accurately measured amount of freeze-dried PTX formulation in phosphate buffered saline (PBS, pH 7.4) and transferring the suspension into dialysis membrane cassettes (Slide-A-Lyzer G2, Thermo Scientific, Rockford, IL) with a molecular weight cut-off of 3500 Da. The cassettes containing PTX nanosuspensions were submerged in PBS buffer solution at 37±1 °C in an incubator under constant shaking(100 rpm). Sink conditions were maintained: the maximum theoretical concentration of the dissolved drug was < 1 % of the saturation concentration. At predetermined intervals, samples were withdrawn from outside the membrane cassettes to be analyzed by HPLC. The volume removed was replaced by fresh buffer. The samples were filtered through a 0.2 μm cellulose acetate filter with low protein binding before the analysis of the drug concentration. The samples were analyzed by HPLC according to the procedure outlined above. Experiments were performed in triplicate.

2.4. *In vitro* cytotoxicity of formulation

Cell culture—Human KB epidermal carcinoma cells and SKOV-3 ovarian cancer cells were obtained from Dr. Yoon Yeo's lab (Purdue University). Cell culture media FA-deficient RPMI-1640 supplemented with 10% fetal bovine serum, 100 U/mL penicillin and 100 μg/mL streptomycin and Dulbecco's Modified Eagle Medium (DMEM) supplemented with 10% (v/v) heat-inactivated fetal bovine serum (FBS) were obtained from Life Technologies Co., Grand Island, NY. Human KB epidermal carcinoma cells were cultured at 37 °C with FA-deficient RPMI-1640in a humidified atmosphere of 5% CO_2 and 90% relative humidity (Nuaire Incubator, Plymouth, MN). The cells were passaged upon reaching approximately 90% confluence from T-flasks using 0.25% trypsin-EDTA (Sigma Aldrich, St. Louis, MO). SKOV-3 ovarian cancer cells were cultured in DMEM at 37 °C under a humidified atmosphere containing 5% CO2. The cells were also passaged upon reaching approximately 90% confluence from T-flasks using 0.25% trypsin-EDTA.

Cytotoxicity study—This method was comparable to those previously reported for *in vitro* cytotoxicity studies. KB cells were seeded in a 96-well plate at a density of 5×10^4 cells /well. SKOV-3 cells were seeded in a 96-well plate at a density of 4×10^5 cells / well. PTX formulation was suspended in buffer at 10 mg/ml and further diluted from 10 mg/ml to 1×10^{-8} mg/ml for measurement. Transferrin solution was also diluted in buffer at the same concentration values. The cells were then exposed to a suspension or solution at 37 °C for 72 hours. After washing once with PBS to remove the samples, a total volume of 20 μl of 5 mg/ml MTT solution was added to each well and the plates were further incubated for 240 minutes at 37 °C in the dark. The culture medium was subsequently discarded, and 150 μl of DMSO was added to dissolve the dark-blue formazan crystals. Cell proliferation and viability were quantified spectrophotometrically by measuring the absorbance of the formazan product at a wavelength of 490 nm using a microplate reader (Bio-Rad Model 550, Bio-Rad, Hercules, CA). Cell viability was calculated using the following equation:

$$Cell\ viability = \frac{Int_s}{Int_{control}} \times 100\%$$

Where Int_s is the absorbance intensity of the cells incubated with the PTX formulations and $Int_{control}$ is the absorbance intensity of the cells incubated with the culture medium only.

2.5. *In vivo* antitumor measurement

Formulation—As a positive control, 30 mg of PTX was dissolved in a 50:50 mixture of Kolliphor® EL (Sigma Aldrich, St. Louis, MO) and ethanol at room temperature. Prior to administration in animals, the stock solution was diluted 1:15 with 0.9% saline solution (sterilized by filtration through 0.2 μm filter) to a final concentration of 2 mg/ml. PTX nanocrystals were also suspended to the same concentration in 0.9% saline for administration.

Animal model—Female nude outbred mice (Tac:Cr: (NCr)-Foxn1 Nu) were obtained from Taconic (Hudson, NY) at 4–5 weeks of age (15–20g)and kept under SPF conditions for 1 week before the study. All of the animal experiments comply with the principles of care and use of laboratory animals and were approved by the Institutional Animal Care and Use Committee of Purdue University. The tumor model was established by subcutaneous injection of 5×10^6 KB cells into the right armpit region of each nude mouse. When tumors had developed to approximately 300 mm^3 (one week after initial inoculation), the KB-bearing mice were randomly divided into 4 groups (n = 6). Saline was used as negative control; the dose was 20 mg/kg for PTX solution or PTX nanosuspension formulation. At

Day 7, 11 and 15 after the cell inoculation, the respective treatments were given intravenously to each animal via the tail vein. Tumor size was monitored every other day with a caliper in two dimensions (length and width). The tumor volume was estimated using the following equation:

$$Tumor\ volume = \frac{length \times (width)^2}{2}$$

The body weight of each mouse was also monitored every other day as an index of systemic toxicity. The mice were euthanized on Day 19 and the tumors were excised and weighed. The tumor inhibition rate was calculated by the following equation:

$$Inhibition\ rate = \frac{W_{control} - W_{treated}}{W_{control}} \times 100\%$$

where $W_{control}$ and $W_{treated}$ are the tumor weights of mice treated by saline and PTX solution or nanosuspension respectively.

2.6. Statistical analysis

Results from *in vitro* cytotoxicity and *in vivo* antitumoral activity experiments were evaluated by the unpaired t-test (between two groups) or one-way ANOVA (between multiple groups) with Tukey's multiple comparison tests. When p-values were less than 0.05, statistical significance was considered achieved.

3. Results and Discussion

3.1. PreparingPTX nanocrystal

The optimization process to obtain stable PTX nanocrystals is described in Figure 1. The optimization of PTX nanocrystals to meet our minimum requirements of less than 300 nm in average particle size and within 20 minutes of processing time is dependent on several parameters. First of all, the selection of solvent is an important factor. Methanol, ethanol, DCM, EA and DMSO were selected for initial assessment based on having at least some degree of miscibility with water, since water was the antisolvent of choice for our applications. Another consideration in selecting these solvents is that PTX has a relatively high solubility in them, which facilitates the formation of smaller particles [36]. Preliminary size characterization results show that DCM, EA and DMSO produced significantly ($p<0.05$) larger PTX nanocrystals compared to methanol and ethanol, with no significant ($p=0.7524$) difference in particle size between methanol and ethanol. The specific values for average particle size and PDI are summarized in Table 1. The tendency for DCM, EA and DMSO to produce larger nanocrystals can be rationalized based on the slow diffusion rate of DCM, EA and DMSO in water (as indicated by the smaller diffusion coefficient values) compared to methanol and ethanol, which favors the formation of a smaller number of crystal nuclei and larger particles during the precipitation process [37]. Ethanol was selected as the solvent of choice for our applications over methanol due to its lower toxicity as classified by ICH Guidelines. While use of methanol should be limited because of its inherent toxicity (limited to 600 ppm or less), ethanol poses a lower risk to human health and can be tolerated up to 5000 ppm per day. The morphology of PTX nanocrystals prepared showed rod-like morphology regardless of type of solvent used.

The concentration of PTX in the solvent phase is another important factor. In the optimization process it was found that 3 mg/ml PTX in ethanol is the optimum concentration

required to meet the minimum requirements. The use of drug concentrations above this level increases particle size (Table 1). When the drug concentration is increased from 3 mg/ml the nanocrystal size increased dramatically. This increase in particle size as the drug concentration in solvent increases has been observed in other studies [38] and is attributed to a higher level of supersaturation that increases particle growth and reduces diffusion rate of crystal nuclei between solvent and antisolvent, both conditions that lead to a larger final particle size [39, 40]. At a lower concentration of 1 mg/ml PTX in solvent, particle size was not significantly different from that of PTX at 3 mg/ml ($p = 0.6553$), which has also been observed in antisolvent precipitation studies involving other drugs [41].

The volume ratio of water to ethanol is also critical to this process. An antisolvent-to-solvent ratio of 20:1 was necessary to achieve stable nanocrystals that met the requirements (Table 1). Below this ratio the particle size increased significantly ($p<0.05$). This has also been observed in numerous other studies [41–43]. A generally accepted explanation is that at a given drug content in the system, the degree of supersaturation is increased when the ratio of antisolvent to solvent is increased. A higher degree of supersaturation leads to a greater nucleation rate, which promotes smaller particle size. At low antisolvent to solvent ratios, the nucleation rate is high but the effect is counteracted by the increase in growth rate due to higher solvent phase ratio, and the kinetics favor overall particle growth. Above antisolvent-to-solvent ratio of 20:1, no further decrease in nanocrystal size was seen. This is most likely due to the equilibrium between nucleation and growth processes [44].

A final consideration is the use of hydrophilic polymers or surfactants that may improve physical stability of nanocrystals [45]. Interestingly, in most cases the presence of polymers and surfactants in the antisolvent phase resulted in an increase in nanocrystal size compared to pure water alone as the antisolvent (Table 1).A possible explanation is that the presence of polymers and surfactants in the antisolvent increased the solubility of the drug in water. The solubility enhancing effect of surfactants and polymers has been commonly observed in the formulation of poorly water-soluble drugs [46, 47]. The enhancement of drug solubility in the antisolvent phase reduces the solubility difference between the drug in the solvent and the antisolvent phases, which may be associated with a decrease in the rate of precipitation. In addition, increased solubilization could play a role in enhancing particle growth by Ostwald ripening, since this process is heavily dissolution-dependent. An alternative explanation is that the stabilizers decrease electrostatic repulsion between drug crystals by either adsorbing to the surface of nanocrystals and / or altering the dielectric constant of the liquid medium [48]. In this study, HPMC, PVP and Pluronic® F68 resulted in significant reductions (less negative) ZP compared to the control; however PEG400, Tween® 20 and SDS all had greater ZP values (more negative) but still resulted in bigger nanocrystals. Clearly electrostatic repulsion cannot fully explain why the use of polymers and surfactants increased particle size. Regardless, no stabilizer was used during the preparation of the PTX nanocrystals.

In summary, we found that 3 mg/ml PTX solution in ethanol introduced into an aqueous antisolvent phase at a ratio of 1:20 was critical to achieving stable PTX nanocrystals after 10 minutes of processing at a stirring speed of 1200 rpm augmented with sonication.

3.2. Development of stable formulation

The optimized process described above resulted in the production of PTX nanocrystals suspended in an aqueous medium. For practical applications, it is more beneficial to have the PTX nanocrystals in dried form. Upon further processing to collect and dry the PTX nanocrystals, it was found that the average particle size of PTX nanocrystals increased by 115±10% after centrifugation and drying. This was expected, as during the centrifugation process particles are brought into close proximity that facilitate collision and particle

'sticking', a process that ultimately resulted in particle aggregation and size increase. Clearly, excipients need to be added to prevent particle aggregation from occurring. In preliminary assessments, human serum was found to effectively inhibit PTX nanocrystal size increase during subsequent centrifugation and drying procedures compared to the control. In addition, the presence of serum also inhibited PTX nanocrystal aggregation for at least 7 days in a buffer environment. It is possible that serum proteins formed a stabilizing layer on the surface of the nanocrystals that prevented particle collision and formed larger particles. However, due to the complexity of human serum proteasome [32], it would be more significant for practical applications if one or two specific serum protein or proteins can be identified for their ability to stabilize the PTX nanocrystals. While it is beyond the scope of this work to isolate every single serum protein and individually investigate their ability to stabilize PTX nanocrystals, a more manageable approach was taken, whereby serum proteins were fractionated into several large categories, and each category was investigated for their contribution towards PTX nanocrystal stabilization. Fractions with high levels of effect are then studied further.

Using the modified cold ethanol protein precipitation method outlined in the 'Methods' section, the serum was successfully separated into 4 fractions, designated Fractions I–IV herein this manuscript. The SDS-PAGE analysis of the 4 fractions is demonstrated in Figure 2. Based on these data, several observations can be made. First, fractions I – IV all contained varying amounts of human serum albumin (HSA), the most abundant plasma protein in the blood. The presence of HSA in all fractions was expected due to the abundance of this protein in the serum [1]. The band above HSA around 80 kDa is most likely Trf, which is present in fractions I and IV but not fractions II and III. With the exception of fraction IV, all other fractions also display a very faint band at 25 kDa that is most likely the γ globulin light chain. Fraction I and III also show broad bands at a high molecular weight of around 150 kDa that suggest the presence of immunoglobulin G (IgG). It is noted that there are overlaps in major components of fractions identified from this experiment. This is most likely due to the limited ability to control pH and ionic strength, since in this particular fractionation method, minute deviations in these parameters may lead to huge differences in the types of proteins being precipitated. However, this was not deemed unacceptable for this particular study since the end goal was to simply separate the serum into several different fractions in some way such that each fraction can be monitored for interaction with PTX nanocrystals individually.

The fractions from above displayed a different degree of size change inhibition in PTX nanocrystals (Figure 3). Fraction IV was the most effective at inhibiting particle size increase during subsequent centrifugation and drying, with a size increase of 34.5±5.9% compared to 69.0±10.9% for fraction I, 71.4±12.5% for fraction II and 69.4±8.9% for fraction III. Based on the SDS-PAGE analysis, it can be seen that the major protein components of fraction IV are HSA and Trf, as indicated by strong bands around ~64 kDa and ~80 kDa. Interestingly, fraction I also displays strong bands around these molecular weights, indicating the presence of HSA and Trf as well. However, in presence of similar concentrations of fraction I and IV, PTX nanocrystal size change was significantly higher ($p<0.05$) in I than in IV.It is possible that the presence of Ig (which is present in greater amounts in fraction I but not in IV) and in particular IgG had the opposite effect on PTX nanocrystal stabilization, leading to aggregation that counteracted the stabilizing effect of HSA and Trf.

To study this result further, the effect of HSA, Trf and IgG were examined individually. The results are presented in Table 2. In general, for both HSA and Trf, the ability to stabilize PTX nanocrystals shows a concentration dependent effect. Increasing protein concentration decreased the extent of PTX nanocrystal size change. The presence of higher concentrations

of HSA or Trf may have resulted in increased viscosity of the fluid, which may act to hinder PTX nanocrystal diffusion and reduce the nanocrystals' ability to collide into one another to form larger particles. Furthermore, it is highly possible that the adsorption of HSA or Trf molecules on the surface of PTX nanocrystals acted as a barrier to prevent nanocrystals from aggregation. The data displayed in Table 2 shows that Trf was the most effective stabilizer of PTX nanocrystals when similar concentrations of Trf and HSA were used. By the addition of 4 mg/ml Trf solution to PTX nanocrystals the average size increased by only 5.57±2.7% after centrifugation and drying. The increase in particle diameter of approximately 16 nm (or 8 nm in radius) corresponds well with the dimension of a single layer of Trf molecules [49]. The results imply that the adsorption of Trf to PTX nanocrystals most likely resulted in better stabilization of particles during subsequent processing due to the larger size of the Trf protein compared to HSA (~4 nm in monolayer thickness [30]) which can be rationalized based on the increased distance between particles and steric effects. Furthermore, Trf content in the formulation is also significantly higher than HSA, which could be attributed to a higher amount of Trf being pelleted during the centrifugation process due to its higher molecular weight. This may also have increased PTX nanocrystal stability in the nanosuspension.

On the other hand, the data seem to suggest that IgG induces particle aggregation. When IgG solution was added to PTX nanocrystals, the measured particle size of the formulation increased more than the samples processed without IgG present. However, the dramatic increase in measured particle size is most likely influenced by the aggregation of IgG proteins rather than PTX nanocrystals, as seen in the control where pure IgG solution without PTX nanocrystals was processed and subsequent particle size measurement also showed a significant size increase. The tendency for immunoglobulins to aggregate as a result of agitation has been demonstrated elsewhere [50]. To prevent IgG aggregation, suggested strategies include lowering pH and addition of organic osmolytes such as sucrose at a concentration of 10 %. When an IgG solution with a pH at 4.5 was used in the formulation, increase in particle size was reduced significantly. The particles were very well-stabilized when 10 % sucrose was added to the IgG solution, with almost no change in particle size after processing. The results above suggest that IgG can be an effective stabilizer for PTX nanocrystals if immunoglobulin aggregation can be prevented.

Based on the results and discussion above, Trf was selected as the stabilizer serum protein of choice for PTX nanocrystals.

3.3. Characterization of formulation

X-ray diffractograms of PTX-Trf in comparison with the drug alone, PTX nanocrystals and the physical mixture of the drug and Trf are shown in Figure 4. Average particle size for the PTX-Trf formulation was 303.5 nm with PDI of 0.239.The addition of Trf increased average particle size slightly with no significant influence on PDI of resultant particles. The increase in particle diameter of approximately 16 nm (or 8 nm in radius) corresponds well with the dimension of a single layer of Trf molecules [49]. Drug content of the PTX-Trf formulation was approximately 55–60%as determined by HPLC analysis. The crystallinity of PTX is confirmed with retention of characteristic peaks in X-ray diffractograms.Dominant peaks at 2θ angles between 4° and 7° and between 10° and 15° were still observed in PTX formulations (nanocrystals with and without Trf).The X-ray diffraction patterns were superimposable for the formulation tested before and after 3 months' storage at 4 °C, which implies that no physical form changes had taken place during the storage period.

The stability of the formulation was also confirmed with particle size, PDI and ZP measurements taken at 1 month intervals throughout the storage period. Particle size, PDI and ZP of the PTX-Trf formulationduring 3 months' storage at 4 °C are shown in Table 3.

The formulation was also imaged by SEM and AFM to confirm particle size reported by dynamic light scatterin g (DLS), since DLS approximates particle size by measuring the diffusion coefficient and is therefore more accurate when used to measure particle sizes of spherical particles. Manual measurements taken from SEM and AFM images showed an average particle size of 277.8 ± 23.9 nm, which is closely reflected in DLS measurements. Particle size, PDI and ZP showed no significant changes over the period of 3 months. The maintenance of average particle size and PDI precludes the possibility that Ostwald ripening took place.

The dissolution profiles of PTX and its respective formulations (nanocrystal with or without Trf) were evaluated in PBS at pH 7.4. As shown in Figure 5, both PTX nanocrystals and PTX-Trf formulations showed significantly higher dissolution rates in comparison to the control. More than 20% and 35% of PTX nanocrystals and PTX-Trf were released within 50 hours, respectively, whereas less than 5% release was achieved after 50 hours for PTX as received from the manufacturer. The increased rate of dissolution is likely due to the small size and large surface area of PTX nanocrystals as predicted by the Noyes-Whitney equation. According to this equation, dissolution velocity dC / dt is proportional to the concentration gradient $A(C_s - C_x)/h$, where A is the surface area of the solid, Cs is the concentration of the solid in the diffusion layer, Cx is the bulk concentration of the solid and h is the diffusion layer thickness [51]. The nanonization of the drug particles leads to large increase in particle surface area, which leads to increased dissolution velocity. An additional effect of nanonization is reduced diffusion layer thickness, which also contributes to an increase in the dissolution rate. This is in agreement with our experimental dissolution results. Rather interestingly, the Trf formulation showed a lower dissolution rate compared to pure PTX nanocrystals. A possible explanation is the binding of Trf to molecular forms of PTX which prevented passage of PTX molecules from within the membrane cassette to the surrounding medium. This may potentially be beneficial for the delivery of PTX nanocrystals in chemotherapy because it may prolong circulation and premature loss of PTX.

3.4. *In vitro* cytotoxicity of PTX formulations

Cytotoxicity of PTX formulations was evaluated in cancerous KB and SKOV-3 cell lines. The half maximal inhibitory concentrations (IC50) were determined from the concentration-dependent cell viability curves as shown in Figure 6. For pure PTX nanosuspensions, the IC50 were on the scale of 1.0 E-5 mg/ml in KB cells and 1.0 E-4 mg/ml in SKOV-3 cells respectively. For PTX-Trf nanosuspension, the IC50 values were on the same order of magnitude. There was no statistically significant difference between the IC50 values of PTX nanosuspension and PTX-Trf nanosuspension in both cell lines. The concentration-dependent cell viability curves for PTX and PTX-Trf were virtually superimposable. The similar cytotoxicity profile can be explained based on the fact that both PTX nanocrystals and PTX-Trf were incubated with the cells for 72 hours before being subjected to a MTT assay and analyzed for results. As such both PTX nanocrystals and PTX-Trf were likely to be dissolved in the medium due to the small size of particles, leading to similar cytotoxic performance overall. In comparison, the IC50 data seems to suggest that PTX and PTX-Trf nanosuspension formulations were more potent against KB cells than SKOV-3 cells. It is possible that the difference in response is due to differences in cell line properties. To the best of our knowledge, no other studies have compared potency of PTX and PTX-based formations across these cell lines. Further study may be needed to clarify this difference, which is outside the scope of the current study.

3.5. *In vivo* antitumor effect of PTX formulations

At a dose of 20 mg/kg, PTX solution, PTX nanosuspension and PTX-Trf nanosuspension were administered to each KB bearing mouse via tail vein on Day 7, 11 and 15 after initial tumor cell inoculation. As a negative control, saline solution was also given via the tail vein to mice in the control group in the same manner. The tumor progression results are shown in Figure 7. The data indicates that both PTX nanosuspension and PTX-Trf nanosuspension yielded significant tumor inhibition in comparison to the negative control group. In particular, the treatment from PTX-Trf was significantly better at inhibiting tumor volume change compared to PTX nanosuspension. This is thought to be due to increased stability of PTX-Trf, resulting in enhanced blood circulation in comparison with the control PTX nanocrystals that aggregate in blood. Calculated tumor inhibition rates based on the averaged weight of tumors dissected from the animals were 28.8% and 45.1% for PTX and PTX-Trf nanosuspension treatment groups, respectively. The tumor inhibition rates between these two groups were significantly different from each other ($p<0.001$). Combined with the tumor progression results, the data indicate better treatment efficacy for PTX-Trf compared to PTX alone. The results can be attributed to the presence of Trf in the formulation, which may have played a role in stabilizing PTX nanocrystals as well as facilitated PTX accumulation due to the presence of Trf receptors on surface of KB cells.

Interestingly, PTX solution in a 50:50 mixture of Cremophor EL and ethanol showed significantly better tumor volume inhibition compared to both the other positive treatment groups. By 12 days after initial injection, the average tumor volume in PTX solution treated mice, had reached 257.1mm^3 compared to 1,455 mm^3 and 1,176 mm^3 for PTX nanocrystal and PTX-Trf formulation, respectively. The calculated tumor inhibition rate was 93.3% for the PTX solution. This value was significantly ($p<0.001$) higher than the PTX-Trf and the PTX nanosuspensions. However, while the antitumor efficacy of Taxol® was higher, its toxicity was also significantly higher compared to the control and PTX nanocrystal formulations. This is indicated in Figure 8, where the average body weight of mice over time is shown. During the first 2 days, the average weight of mice treated by Taxol® decreased by approximately 3.89% compared to an increase of 0.03% for the control and small decreases of 0.58% and 0.29% for PTX nanocrystal and PTX-Trf formulations, respectively. The high efficacy of Taxol in tumor growth inhibition has been observed in a previous study utilizing KB cells as a model cell line [52]. This superior efficacy has been attributed to the presence of Cremophor that forms micelles small enough to penetrate deeper into the tumor mass compared to bigger nanocrystals [53, 54]. Studies have observed that Taxol accumulates at a significantly higher extent compared to nanocrystals, which may have led to the higher tumor inhibitory effect seen in the present study [55]. This suggests that the amount of PTX-Trf accumulated at the tumor site may be between those of Taxol and PTX nanocrystals. But the quantity is around 1% of the total administered dose [55], and at that level, the anti-tumor effect may be mainly due to PTX that is absorbed into the tumor cells, rather than the amount deposited near tumor. This makes sense, since Taxol provide better PTX solubility than PTX-Trf, which in turn provides better solubility than PTX nanocrystals which are prone to aggregate. Although the efficacy of Taxol was greater here, its toxicity was also higher, which is a common concern that limits its usage. In comparison, the PTX-Trf formulation demonstrated reasonable tumor inhibitory effect with minor toxicity issues compared withthe control. The reduced toxicity by the nanocrystal formulation may be significant enough for clinical applications, as demonstrated by the Doxil® formulation [56]. The ultimate goal of PTX-Trf approach is to develop a formulation that is as effective as or better than Taxol, but with lower toxicity. Such a goal can be achieved through further improvement and optimization of nanocrystal properties, e.g., nanocrystal size and Trf coating, which can affect biodistribution of PTX.

4. Conclusion

In the current study, a PTX nanocrystal formulation based on stabilization with Trf was successfully developed. To ourknowledge, the approach of non-covalently modifying anticancer drug nanocrystals with serum protein taken in this study has yet to be employed elsewhere. Stable nanoparticles (less than 350 nm) containing PTX and Trfwere prepared in a simple manner without complex chemical reactions. The non-covalently modified PTX formulation was found to be stable over at least 3 months at 4 °C. *In vivo* antitumor activities of PTX were significantly enhanced by the addition of Trf in comparison to just the PTX nanocrystal alone. Overall, this study suggests the potential benefit of using a serum protein in a non-covalent manner in conjunction with PTX nanocrystalsas a promising drug delivery model for anticancer therapy, especially with reduced side effects.

Acknowledgments

This work was supported by the Showalter Research Trust Fund and the National Institute of Health through CA129287, GM095879 and HL062552.

References

1. Miele E, Spinelli GP, Tomao F, Tomao S. Albumin-bound formulation of paclitaxel (Abraxane (R) ABI-007) in the treatment of breast cancer. International Journal of Nanomedicine. 2009; 4:99–105. [PubMed: 19516888]
2. Schiff PB, Horwitz SB. Taxol stabilizes microtubules in mouse fibroblast cells. Proceedings of the National Academy of Sciences of the United States of America-Biological Sciences. 1980; 77:1561–1565.
3. Rowinsky EK, Cazenave LA, Donehower RC. Taxol - a novel investigational antimicrotubule agent. Journal of the National Cancer Institute. 1990; 82:1247–1259. [PubMed: 1973737]
4. Schiff PB, Fant J, Horwitz SB. Promotion of microtubule assembly in vitro by Taxol. Nature. 1979; 277:665–667. [PubMed: 423966]
5. Yoncheva K, Calleja P, Agueros M, Petrov P, Miladinova I, Tsvetanov C, Irache JM. Stabilized micelles as delivery vehicles for paclitaxel. International Journal of Pharmaceutics. 2012; 436:258–264. [PubMed: 22721848]
6. Deepa G, Ashwanikumar N, Pillai JJ, Kumar GSV. Polymer Nanoparticles - A Novel Strategy for Administration of Paclitaxel in Cancer Chemotherapy. Current Medicinal Chemistry. 2012; 19:6207–6213. [PubMed: 22834822]
7. Sartori S, Caporale A, Rechichi A, Cufari D, Cristallini C, Barbani N, Giusti P, Ciardelli G. Biodegradable paclitaxel-loaded microparticles prepared from novel block copolymers: influence of polymer composition on drug encapsulation and release. Journal of Peptide Science. 2013; 19:205–213. [PubMed: 23495215]
8. He HM, Chen S, Zhou JZ, Dou Y, Song L, Che L, Zhou X, Chen X, Jia Y, Zhang JX, Li SH, Li XH. Cyclodextrin-derived pH-responsive nanoparticles for delivery of paclitaxel. Biomaterials. 2013; 34:5344–5358. [PubMed: 23591391]
9. Wang HB, Cheng G, Du Y, Ye L, Chen WZ, Zhang LM, Wang TW, Tian JW, Fu FH. Hypersensitivity reaction studies of a polyethoxylated castor oil-free, liposome-based alternative paclitaxel formulation. Molecular Medicine Reports. 2013; 7:947–952. [PubMed: 23291923]
10. Xia XJ, Guo RF, Liu YL, Zhang PX, Zhou CP, Jin DJ, Wang RY. Formulation, Characterization and Hypersensitivity Evaluation of an Intravenous Emulsion Loaded with a Paclitaxel-Cholesterol Complex. Chemical & Pharmaceutical Bulletin. 2011; 59:321–326. [PubMed: 21372412]
11. Lv PP, Wei W, Yue H, Yang TY, Wang LY, Ma GH. Porous Quaternized Chitosan Nanoparticles Containing Paclitaxel Nanocrystals Improved Therapeutic Efficacy in Non-Small-Cell Lung Cancer after Oral Administration. Biomacromolecules. 2011; 12:4230–4239. [PubMed: 22044456]
12. Rowinsky EK. Drug therapy - Paclitaxel (Taxol). New England Journal of Medicine. 1995; 333:75–75.

13. Gelderblom H, Verweij J, Nooter K, Sparreboom A. Cremophor EL: the drawbacks and advantages of vehicle selection for drug formulation. European Journal of Cancer. 2001; 37:1590–1598. [PubMed: 11527683]

14. Weiss RB, Donehower RC, Wiernik PH, Ohnuma T, Gralla RJ, Trump DL, Baker JR, Vanecho DA, Vonhoff DD, Leylandjones B. Hypersensitivity reactions from taxol. Journal of Clinical Oncology. 1990; 8:1263–1268. [PubMed: 1972736]

15. Gianni L, Kearns CM, Giani A, Capri G, Vigano L, Locatelli A, Bonadonna G, Egorin MJ. Nonlinear pharmacokinetics and metabolism of paclitaxel and its pharmacokinetic/pharmacodynamic relationships in humans. Journal of Clinical Oncology. 1995; 13:180–190. [PubMed: 7799018]

16. Patravale VB, Date AA, Kulkarni RM. Nanosuspensions: a promising drug delivery strategy. Journal of Pharmacy and Pharmacology. 2004; 56:827–840. [PubMed: 15233860]

17. Gao L, Zhang DR, Chen MH. Drug nanocrystals for the formulation of poorly soluble drugs and its application as a potential drug delivery system. Journal of Nanoparticle Research. 2008; 10:845–862.

18. Rabinow BE. Nanosuspensions in drug delivery. Nature Reviews Drug Discovery. 2004; 3:785–796.

19. Muller RH, Jacobs C, Kayser O. Nanosuspensions as particulate drug formulations in therapy Rationale for development and what we can expect for the future. Advanced Drug Delivery Reviews. 2001; 47:3–19. [PubMed: 11251242]

20. Merisko-Liversidge E, Liversidge GG, Cooper ER. Nanosizing: a formulation approach for poorly-water-soluble compounds. European Journal of Pharmaceutical Sciences. 2003; 18:113–120. [PubMed: 12594003]

21. Peters K, Leitzke S, Diederichs JE, Borner K, Hahn H, Muller RH, Ehlers S. Preparation of a clofazimine nanosuspension for intravenous use and evaluation of its therapeutic efficacy in murine Mycobacterium avium infection. Journal of Antimicrobial Chemotherapy. 2000; 45:77–83. [PubMed: 10629016]

22. Kawakami K, Yoshikawa T, Moroto Y, Kanaoka E, Takahashi K, Nishihara Y, Masuda K. Microemulsion formulation for enhanced absorption of poorly soluble drugs: I. Prescription design. Journal of Controlled Release. 2002; 81:65–74. [PubMed: 11992679]

23. Liversidge GG, Cundy KC. Particle size reduction for improvement of oral bioavailability of hydrophobic drugs: I. Absolute oral bioavailability of nanocrystalline danazol in beagle dogs. International Journal of Pharmaceutics. 1995; 125:91–97.

24. Pouton CW. Lipid formulations for oral administration of drugs: non-emulsifying, self-emulsifying and self-microemulsifying drug delivery systems. European Journal of Pharmaceutical Sciences. 2000; 11(Supplement 2):S93–S98. [PubMed: 11033431]

25. Keck CM, Muller RH. Drug nanocrystals of poorly soluble drugs produced by high pressure homogenisation. European Journal of Pharmaceutics and Biopharmaceutics. 2006; 62:3–16. [PubMed: 16129588]

26. Horn D, Rieger J. Organic Nanoparticles in the Aqueous Phase—Theory, Experiment, and Use. Angewandte Chemie International Edition. 2001; 40:4330–4361.

27. Junghanns J, Muller RH. Nanocrystal technology, drug delivery and clinical applications. International Journal of Nanomedicine. 2008; 3:295–309. [PubMed: 18990939]

28. Jiang TY, Han N, Zhao BW, Xie YL, Wang SL. Enhanced dissolution rate and oral bioavailability of simvastatin nanocrystal prepared by sonoprecipitation. Drug Development and Industrial Pharmacy. 2012; 38:1230–1239. [PubMed: 22229827]

29. McClements DJ. Protein-stabilized emulsions. Current Opinion in Colloid & Interface Science. 2004; 9:305–313.

30. Jeyachandran YL, Mielezarski E, Rai B, Mielczarski JA. Quantitative and Qualitative Evaluation of Adsorption/Desorption of Bovine Serum Albumin on Hydrophilic and Hydrophobic Surfaces. Langmuir. 2009; 25:11614–11620. [PubMed: 19788219]

31. Seo JH, Dembereldorj U, Park J, Kim M, Kim S, Joo SW. Facile internalization of paclitaxel on titania nanoparticles in human lung carcinoma cells after adsorption of serum proteins. Journal of Nanoparticle Research. 2012; 14

32. Kratz F, Elsadek B. Clinical impact of serum proteins on drug delivery. J. Control. Release. 2012; 161:429–445. [PubMed: 22155554]
33. Zhang JY, He B, Qu W, Cui Z, Wang YB, Zhang H, Wang JC, Zhang Q. Preparation of the albumin nanoparticle system loaded with both paclitaxel and sorafenib and its evaluation in vitro and in vivo. Journal of Microencapsulation. 2011; 28:528–536. [PubMed: 21702701]
34. Vanoss CJ. On the mechanism of the cold ethanol precipitation method of plasma-protein fractionation. Journal of Protein Chemistry. 1989; 8:661–668. [PubMed: 2610860]
35. Salasoo I. Distribution of rabbit serum proteins in fractionation by cold ethanol method. Analytical Biochemistry. 1967; 20:200-&. [PubMed: 6034993]
36. Smet L, Colin P, Ceelen W, Bracke M, Bocxlaer J, Remon J, Vervaet C. Development of a Nanocrystalline Paclitaxel Formulation for Hipec Treatment. Pharmaceutical Research. 2012; 29:2398–2406. [PubMed: 22555379]
37. Sinha B, Müller RH, Möschwitzer JP. Bottom-up approaches for preparing drug nanocrystals: Formulations and factors affecting particle size. International Journal of Pharmaceutics. 2013
38. Zhang HX, Wang JX, Zhang ZB, Le Y, Shen ZG, Chen JF. Micronization of atorvastatin calcium by antisolvent precipitation process. International Journal of Pharmaceutics. 2009; 374:106–113. [PubMed: 19446766]
39. Wang Z, Chen JF, Le Y, Shen ZG, Yun J. Preparation of ultrafine beclomethasone dipropionate drug powder by antisolvent precipitation. Industrial & Engineering Chemistry Research. 2007; 46:4839–4845.
40. Zhang JY, Shen ZG, Zhong J, Hu TT, Chen JF, Ma ZQ, Yun J. Preparation of amorphous cefuroxime axetil nanoparticles by controlled nanoprecipitation method without surfactants. International Journal of Pharmaceutics. 2006; 323:153–160. [PubMed: 16828244]
41. Dalvi SV, Dave RN. Controlling Particle Size of a Poorly Water-Soluble Drug Using Ultrasound and Stabilizers in Antisolvent Precipitation. Industrial & Engineering Chemistry Research. 2009; 48:7581–7593.
42. Zhao H, Wang JX, Wang QA, Chen JF, Yun J. Controlled liquid antisolvent precipitation of hydrophobic pharmaceutical nanoparticles in a microchannel reactor. Industrial & Engineering Chemistry Research. 2007; 46:8229–8235.
43. Zhang ZB, Shen ZG, Wang JX, Zhao H, Chen JF, Yun J. Nanonization of Megestrol Acetate by Liquid Precipitation. Industrial & Engineering Chemistry Research. 2009; 48:8493–8499.
44. Zhao H, Wang JX, Zhang HX, Shen ZG, Yun J, Chen JF. Facile Preparation of Danazol Nanoparticles by High-Gravity Anti-solvent Precipitation (HGAP) Method. Chinese Journal of Chemical Engineering. 2009; 17:318–323.
45. Van Eerdenbrugh B, Van den Mooter G, Augustijns P. Top-down production of drug nanocrystals: Nanosuspension stabilization, miniaturization and transformation into solid products. International Journal of Pharmaceutics. 2008; 364:64–75. [PubMed: 18721869]
46. Aggarwal AK, Singh S. Physicochemical characterization and dissolution study of solid dispersions of diacerein with polyethylene glycol 6000. Drug Development and Industrial Pharmacy. 2011; 37:1181–1191. [PubMed: 21449824]
47. Yang C, Xu X, Wang J, An Z. Use of the Co-grinding Method to Enhance the Dissolution Behavior of a Poorly Water-Soluble Drug: Generation of Solvent-Free Drug-Polymer Solid Dispersions. Chemical & Pharmaceutical Bulletin. 2012; 60:837–845. [PubMed: 22790815]
48. Zhang H, Hollis CP, Zhang Q, Li T. Preparation and antitumor study of camptothecin nanocrystals. International Journal of Pharmaceutics. 2011; 415:293–300. [PubMed: 21679755]
49. Jiang X, Weise S, Hafner M, Röcker C, Zhang F, Parak WJ, Nienhaus GU. Quantitative analysis of the protein corona on FePt nanoparticles formed by transferrin binding. Journal of The Royal Society Interface. 2010; 7:S5–S13.
50. Serno T, Carpenter JF, Randolph TW, Winter G. Inhibition of agitation-induced aggregation of an IgG-antibody by hydroxypropyl-β-cyclodextrin. Journal of Pharmaceutical Sciences. 2010; 99:1193–1206. [PubMed: 19774651]
51. Butcher JC, Garg S, Kim D, Sharma P. A modified approach to predict dissolution and absorption of polydisperse powders. Pharmaceutical Research. 2008; 25:2309–2311. [PubMed: 18523873]

52. Yang M, Chen J, Cao W, Ding L, Ng KK, Jin H, Zhang Z, Zheng G. Attenuation of nontargeted cell-kill using a high-density lipoprotein-mimicking peptide--phospholipid nanoscaffold. Nanomedicine. 2011; 6:631–641. [PubMed: 21718175]

53. Nakamura J, Nakajima N, Matsumura K, Hyon S. In vivo cancer targeting of water-soluble taxol by folic acid immobilization. Journal of Nanomedicine and Nanotechnology 2. 2011; 106:106–109. 2 (2011).

54. Wang Z, Yu Y, Dai W, Lu J, Cui J, Wu H, Yuan L, Zhang H, Wang X, Wang J, Zhang X, Zhang Q. The use of a tumor metastasis targeting peptide to deliver doxorubicin-containing liposomes to highly metastatic cancer. Biomaterials. 2012; 33:8451–8460. [PubMed: 22940213]

55. Hollis CP, Weiss HL, Leggas M, Evers BM, Gemeinhart RA, Li T. Biodistribution and bioimaging studies of hybrid paclitaxel nanocrystals: lessons learned of the EPR effect and image-guided drug delivery. J. Control. Release. 2013; 172:12–21. [PubMed: 23920039]

56. Barenholz Y. Doxil® - The first FDA-approved nano-drug: Lessons learned. J. Control. Release. 2012; 160:117–134. [PubMed: 22484195]

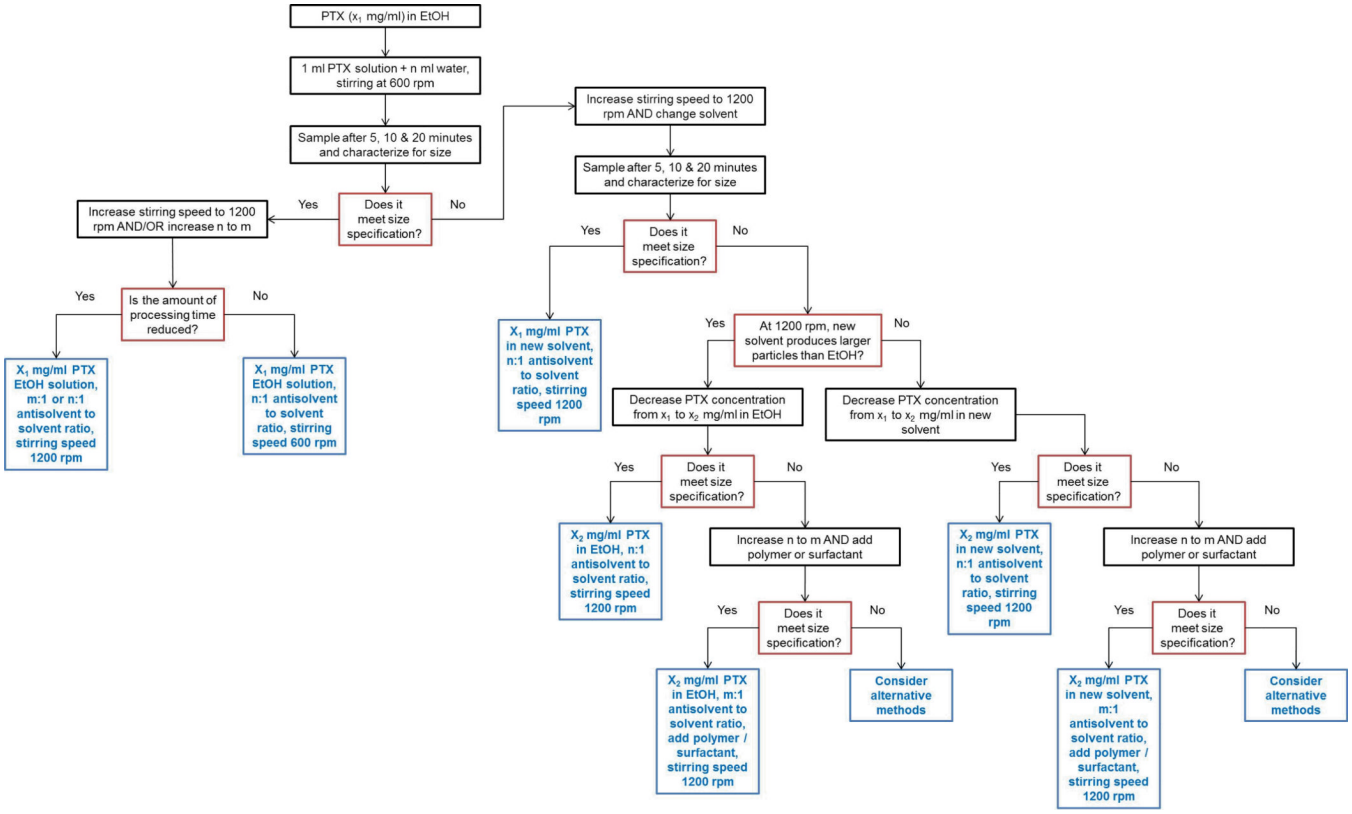

Figure 1.
Flow chart of the parameter optimization process to prepare PTX nanocrystals of desired size.

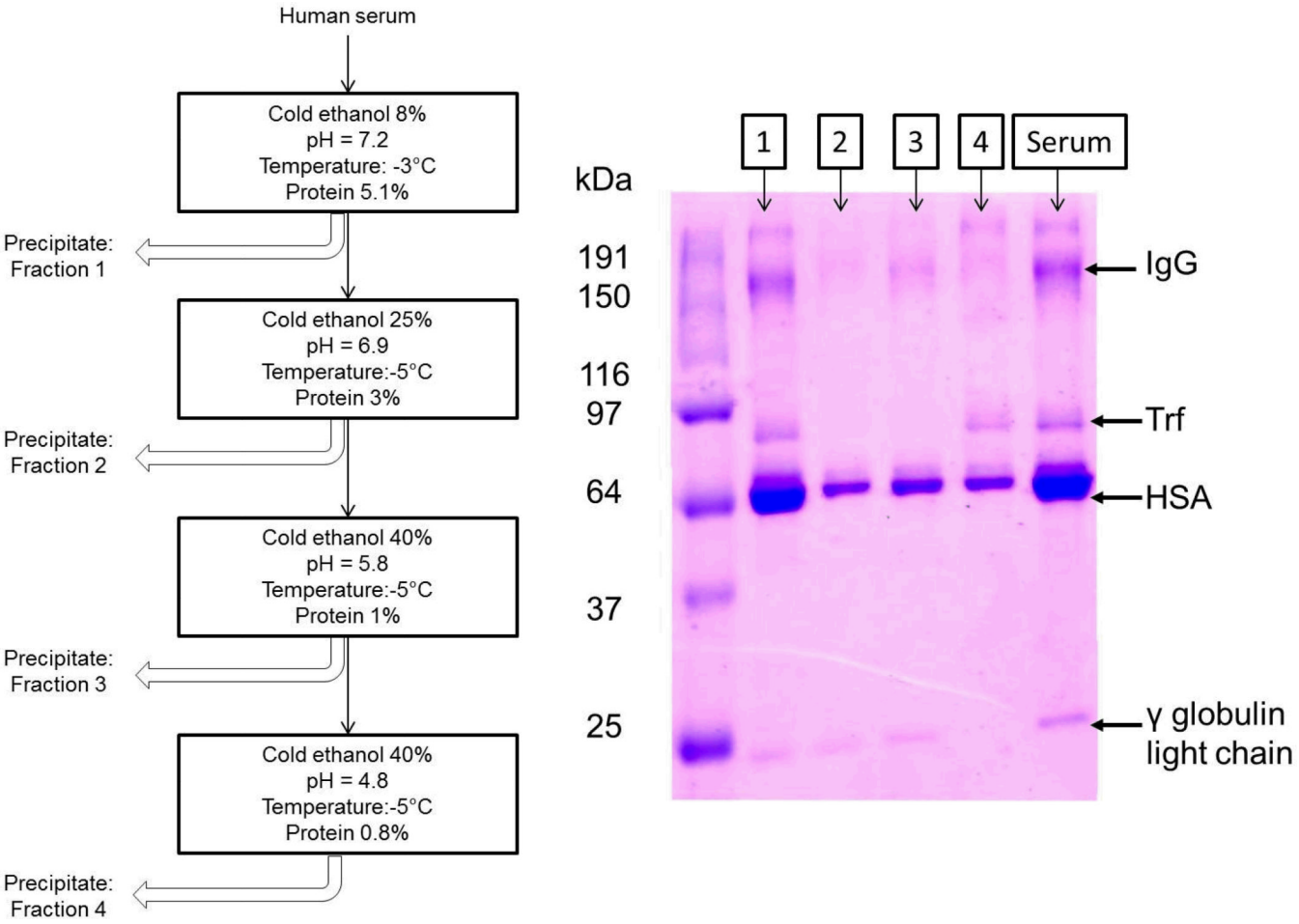

Figure 2.

Overview of the serum fractionation method used and resultant SDS-PAGE analysis of the four different fractions

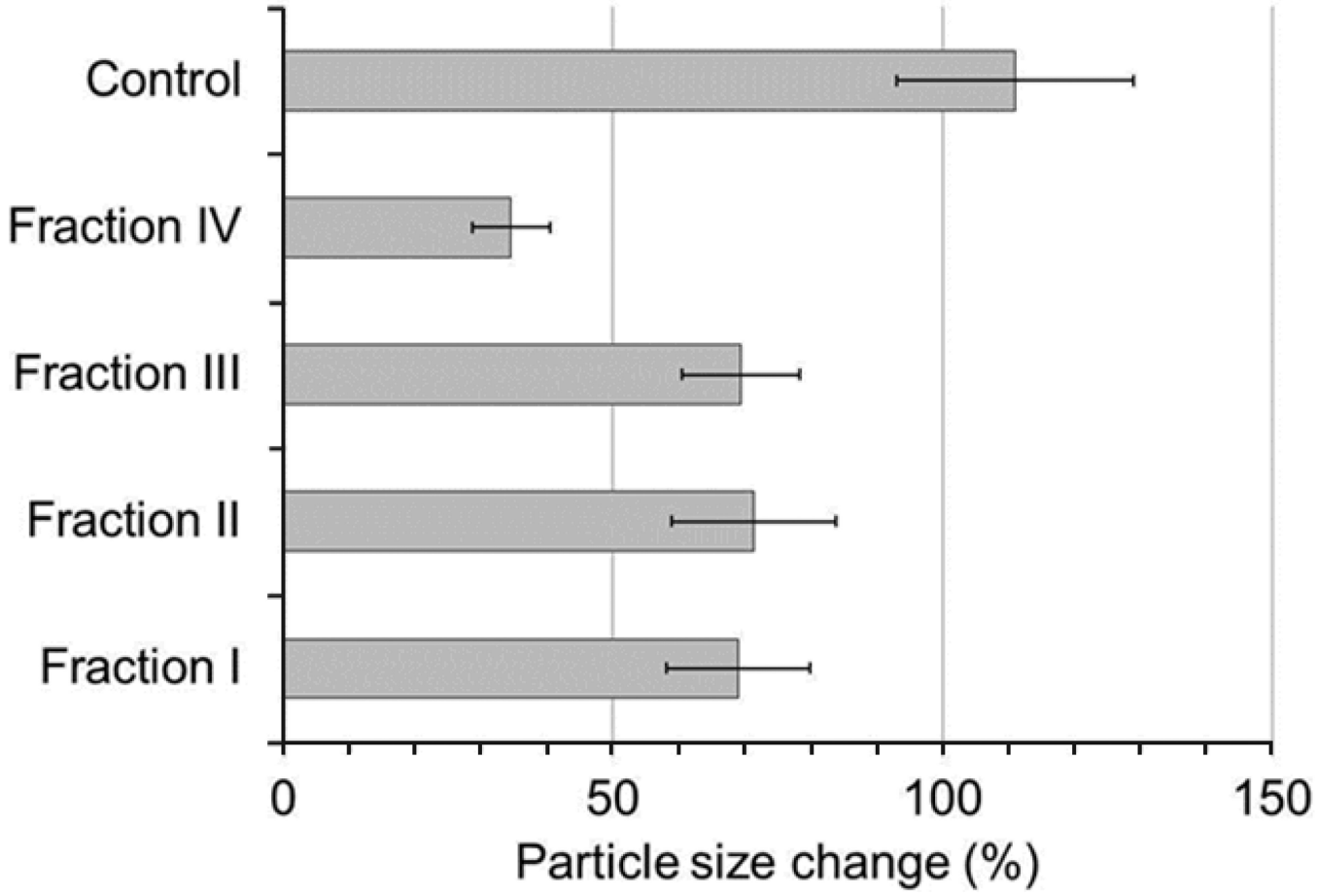

Figure 3.
Effect of various serum protein fractions on PTX size change after incubation and centrifugation.

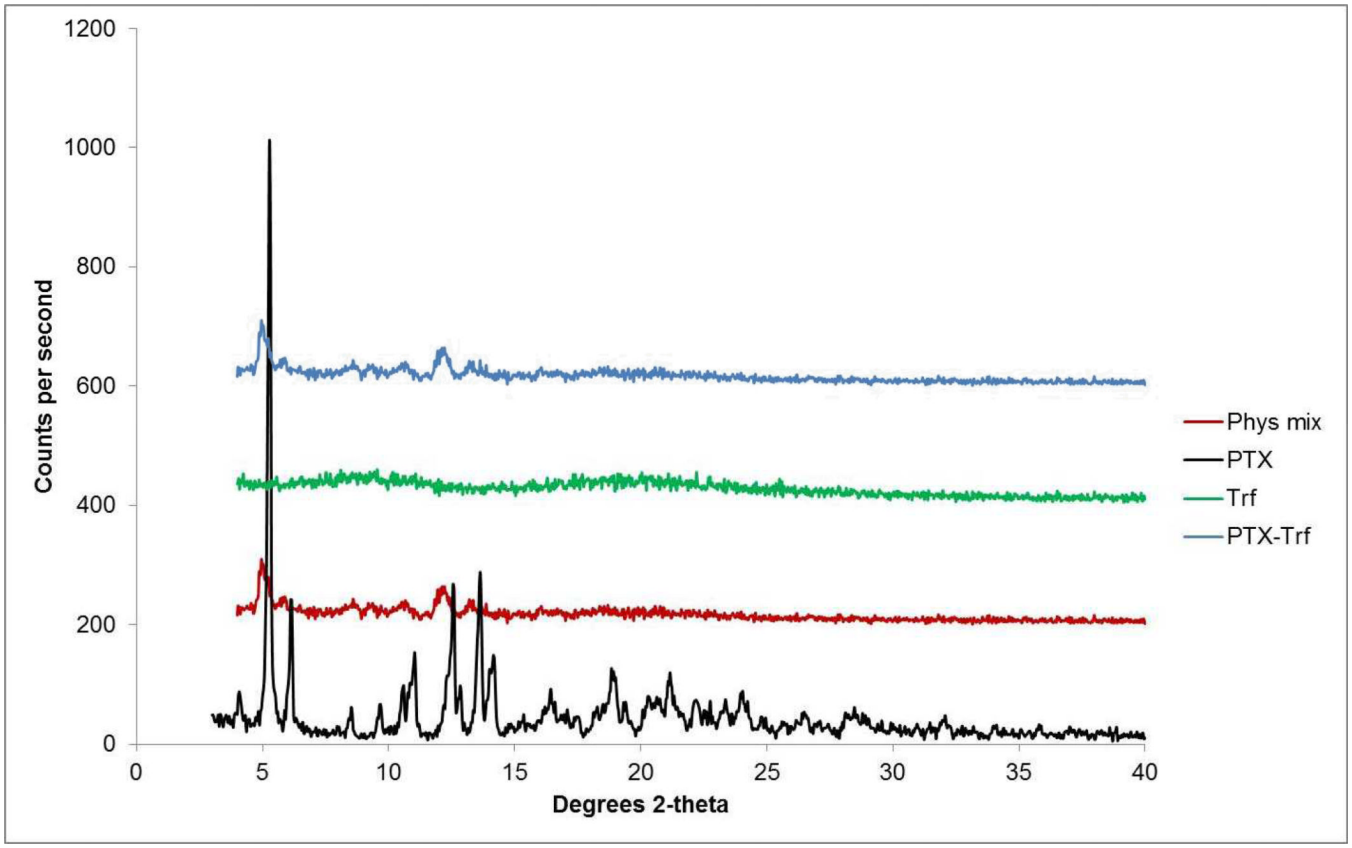

Figure 4.
X-ray diffractogram of pure PTX, Trf, physical mixtures and PTX-Trf formulation.

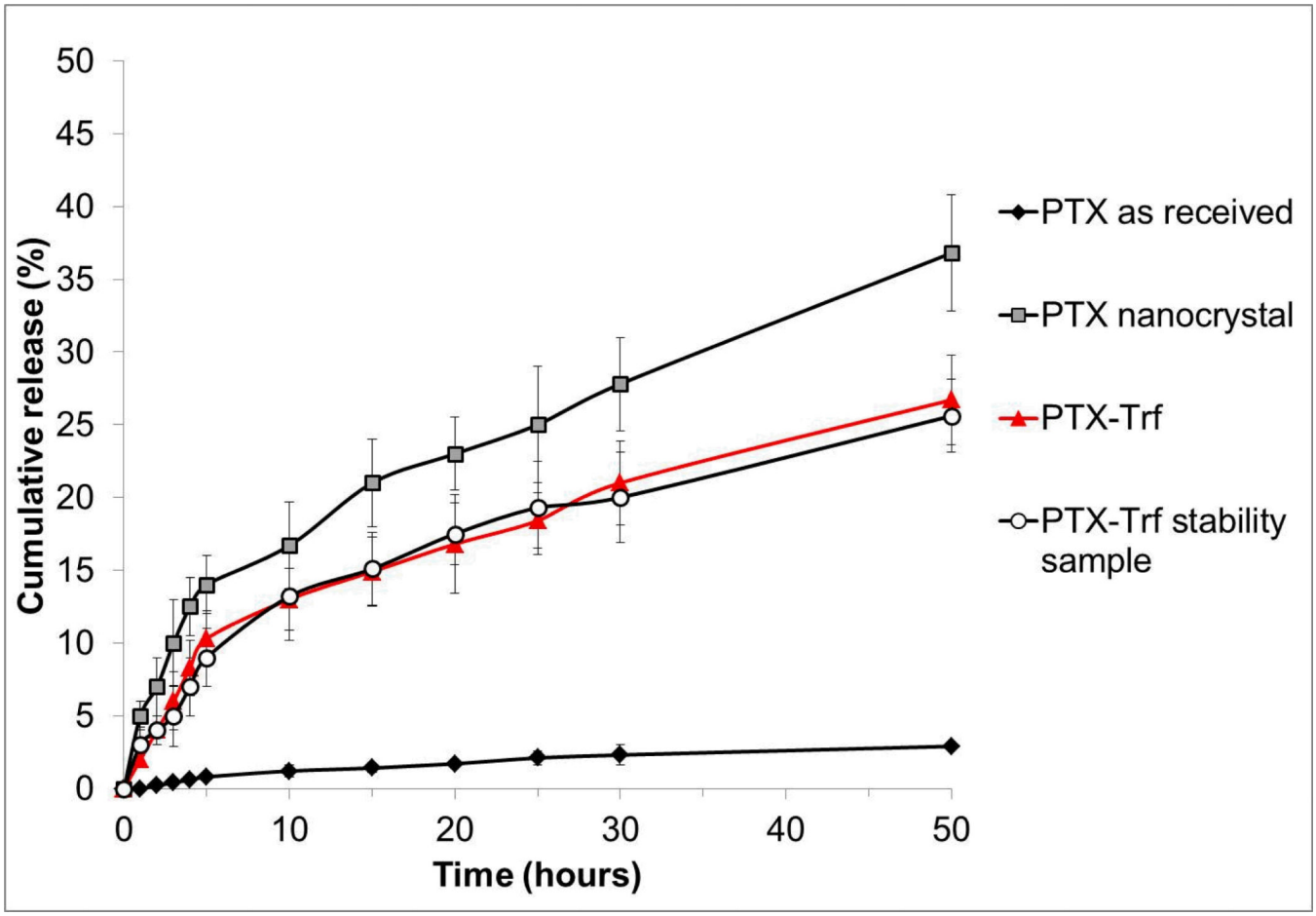

Figure 5.
In vitro release profiles of PTX in phosphate buffer, pH 7.4.

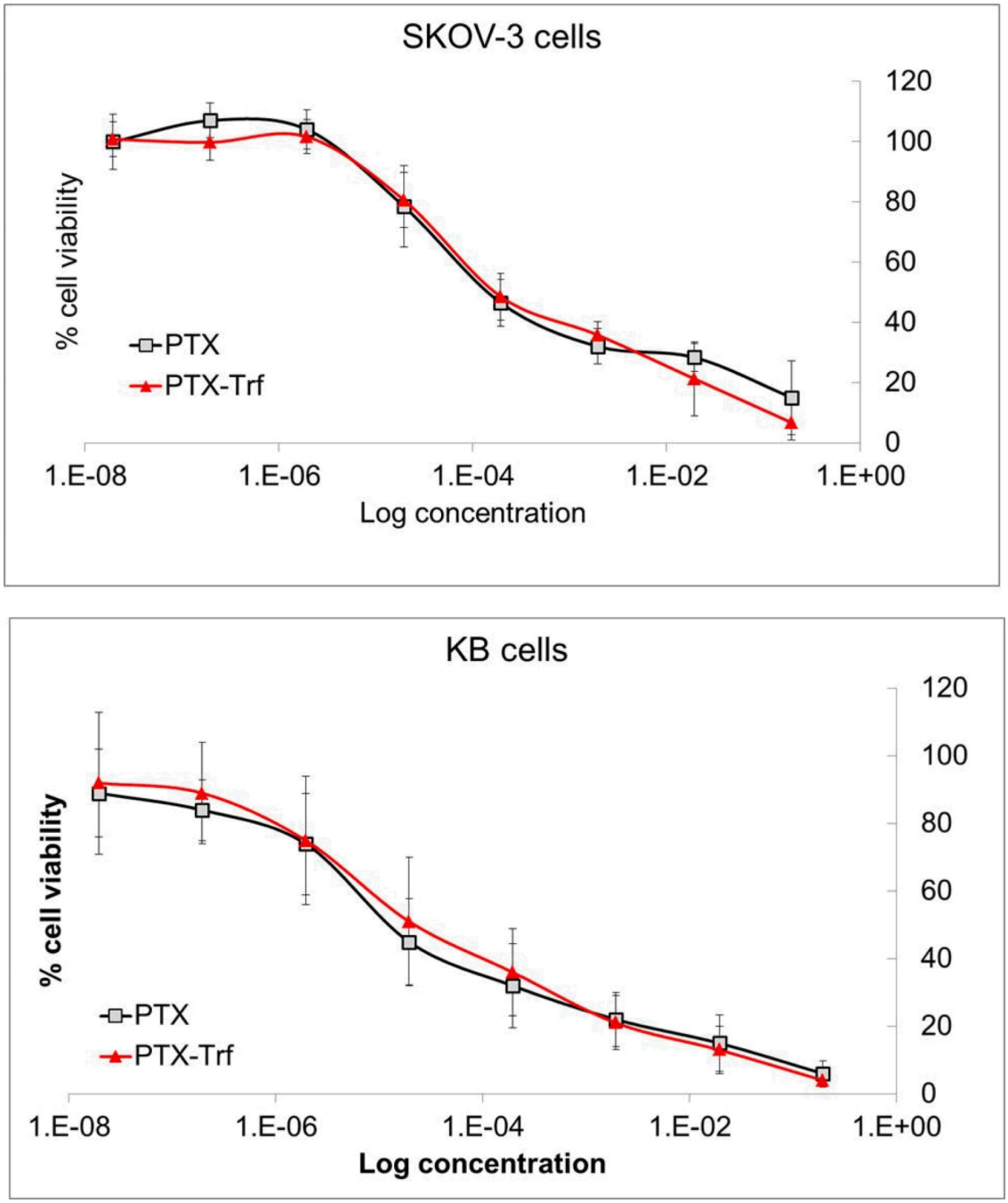

Figure 6.
In vitro cytotoxicity profiles of PTX nanocrystals and PTX-Trf formulation in SKOV-3 and KB cells.

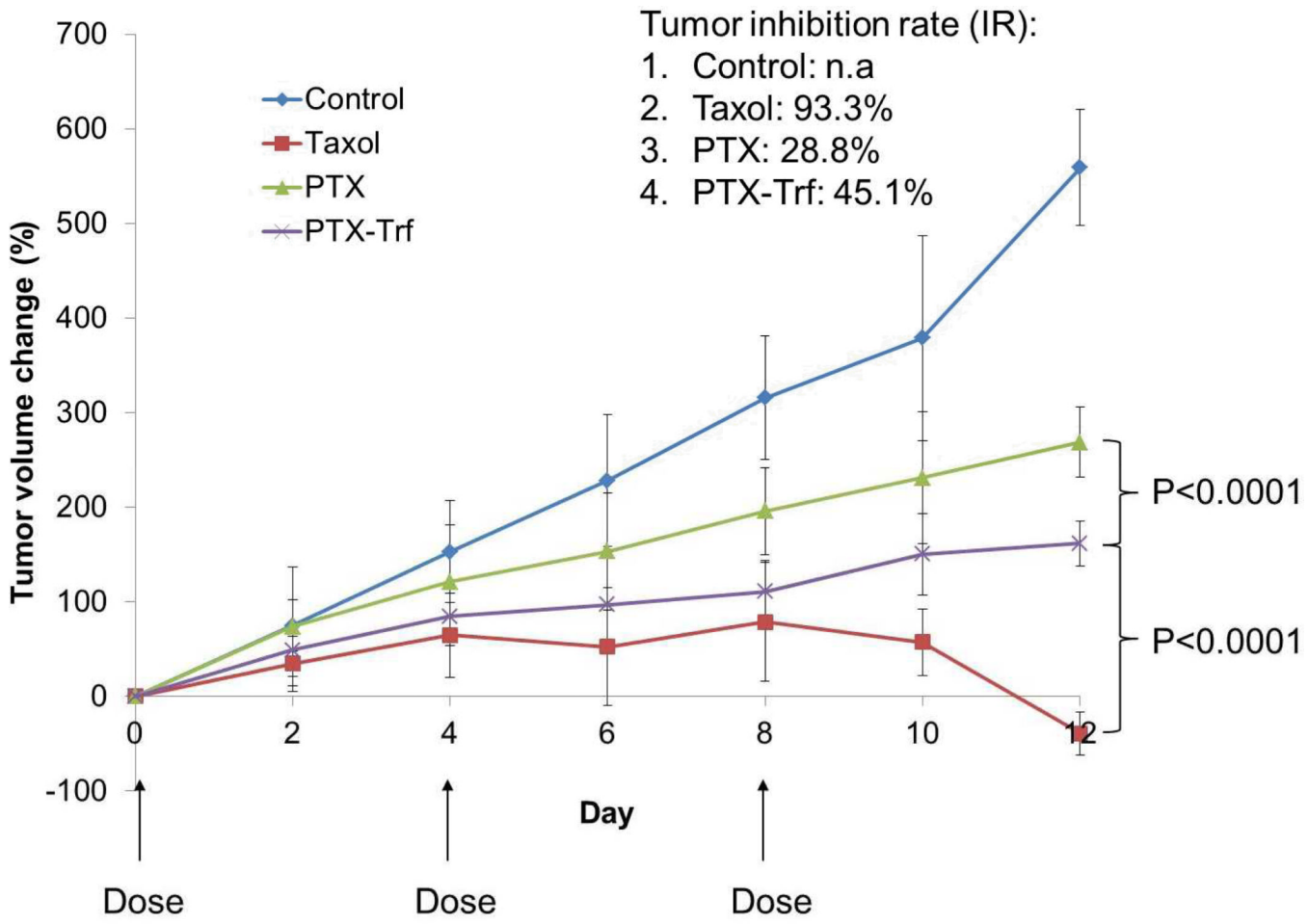

Figure 7.
In vivo antitumor efficacy of PTX formulations in mice.

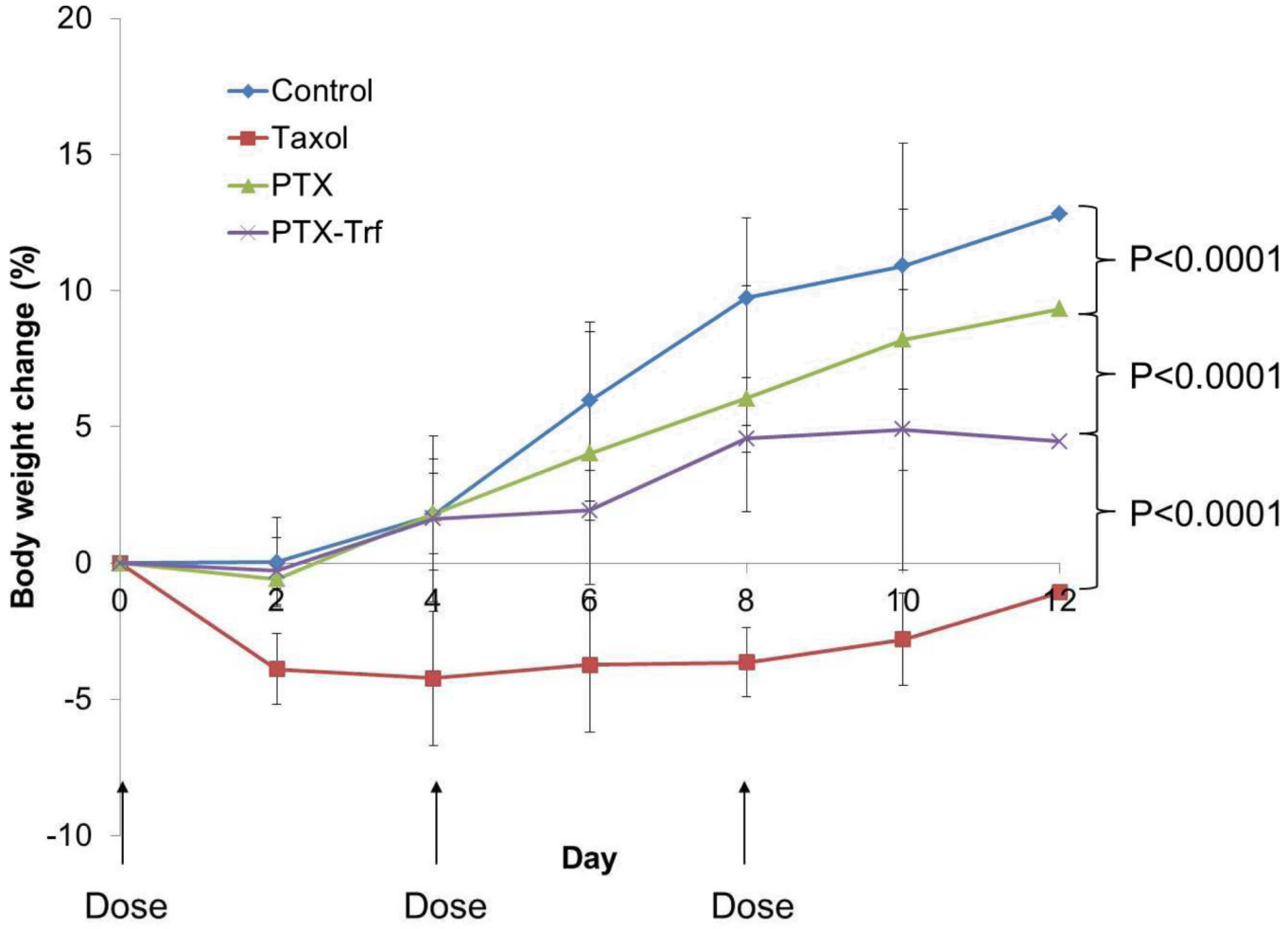

Figure 8.
Body weight change of mice after administration of various PTX formulations.

Table 1

Summary of PTX nanocrystal size and PDI under various processing conditions

		Average particle size (nm)	PDI
Solvent	Ethanol	287± 8	0.20
	Methanol	280±15	0.15
	DCM	338±13	0.09
	EA	418±20	0.20
	DMSO	353±13	0.21
PTX concentration	1 mg/ml	296±12	0.13
	3 mg/ml	268±8	0.20
	5 mg/ml	1,670±89	0.40
	9 mg/ml	4,421±144	0.39
	12 mg/ml	4,358±103	0.32
Antisolvent-solvent ratio	40:1	291±10	0.12
	20:1	287±8	0.20
	10:1	518±19	0.30
	5:1	746±25	0.30
Stabilizer	HPMC	490±19	0.25
	PVP	514±23	0.19
	PEG400	303±11	0.14
	Pluronic F68	330±18	0.20
	Pluronic F127	278±10	0.20
	Tween 20	353±14	0.14
	Tween 80	290±12	0.19
	SDS	379±21	0.17

Table 2

Effect of serum proteins HSA, Trf and IgG on PTX nanocrystal size

	Concentration	Average particle size (nm)	% change from original
HSA	2 mg/ml	443± 24	70
	10 mg/ml	400± 20	54
	20 mg/ml	383± 23	34
	40 mg/ml	352± 25	23
	50 mg/ml	326± 20	13
Trf	3 mg/ml	400± 14	40
	4 mg/ml	304± 13	6
IgG	3 mg/ml	1541 ± 102	437
	10 mg/ml	1825 ± 128	536
	10 mg/ml, pH 4.7	534± 39	86
	10 mg/ml, 10% sucrose	360± 24	26

Table 3

Particle size, PDI and ZP characterizations after storage at 4 °C

Duration	Particle Size (nm)	PDI	Zeta Potential (mV)
0	303 ± 11.1	0.124	− 13.6
1 month	296 ± 13.4	0.136	− 11.8
2 months	305 ± 9.9	0.118	− 13.4
3 months	301 ± 14.2	0.129	−14.7